J Mater Sci: Mater Med (2014) 25:363–373
DOI 10.1007/s10856-013-5076-1

Preparation and evaluation of novel nano-bioglass/gelatin conduit for peripheral nerve regeneration

Masoumeh Foroutan Koudehi · Abbas Ali Imani Fooladi · Kourosh Mansoori · Zahra Jamalpoor · Afsaneh Amiri · Mohammad Reza Nourani

Received: 24 July 2013 / Accepted: 20 October 2013 / Published online: 2 November 2013

Abstract Peripheral nerves are exposed to physical injuries usually caused by trauma that may lead to a significant loss of sensory or motor functions and is considered as a serious health problem for societies today. This study was designed to develop a novel nano bioglass/gelatin conduit (BGGC) for the peripheral nerve regeneration. The bioglass nanoparticles were prepared by sol–gel technique and characterized using transmission electron microscopy (TEM), Fourier transform infrared spectroscopy (FTIR) and X-ray diffraction analysis. The interfacial bonding interaction between the nano-bioglass and gelatin in the developed conduits was assessed by FTIR. The surface morphology and pore size of the nanocomposite were investigated through scanning electron microscopy with the pore size of the conduits being 10–40 μm. Biocompatibility was assessed by MTT assay which indicated the BGGC to have good cytocompatibility. The guidance channel was examined and used to regenerate a 10 mm gap in the right sciatic nerve of a male Wistar rat. Twenty rats were randomly divided into two experimental groups, one with the BGGC and the other being normal rats. The gastrocnemius muscle contractility was also examined at one, two and three months post-surgery in all groups using electromyography (EMAP). Histological and functional evaluation and the results obtained from electromyography indicated that at three months, nerve regeneration of the BGGC group was statistically equivalent to the normal group ($p > 0.05$). Our result suggests that the BGGC can be a suitable candidate for peripheral nerve repair.

M. F. Koudehi
Tissue Engineering Division, Applied Biotechnology Research Center, Baqiyatallah University of Medical Sciences, Tehran, Iran

M. F. Koudehi · A. Amiri
Department of Chemistry, Islamic Azad University, Central Tehran Branch, Tehran, Iran

A. A. I. Fooladi
Applied Microbiology Research Center, Baqiyatallah University of Medical Sciences, Tehran, Iran

K. Mansoori
Physical Medicine and Rehabilitation Department, Iran University of Medical Science, Tehran, Iran

Z. Jamalpoor
Department of Tissue Engineering, School of Advanced Medical Technologies, Tehran University of Medical Sciences, Tehran, Iran

M. R. Nourani (✉)
Nano Biotechnology Research Center, Baqiyatallah University of Medical Sciences, Tehran, Iran
e-mail: r.nourani@yahoo.com

1 Introduction

Trauma injuries are the main cause of peripheral nerve defects which are followed by disabilities. Since there are restrictions using autografts such as limitations in availability of donor site and donor site morbidity, the need to using tissue engineering techniques is increasing.

This condition requires the use of nerve grafts and peripheral nerve substitutes to support the healing process. Autografts have been considered as the gold standard for peripheral nerve repair due to their obvious properties; however there are restrictions in using autografts such as limitations in availability of the donor site, the sensation loss of donor area and donor site morbidity. Allografts, on the other hand, are plentiful in source but in long-term there is a high possibility of tissue rejection due to the

immune system, thus having a lower value in the promotion of nerve regeneration as compared to autografts [1–4]. In the absence of donor tissues, conduits are required for axons to regenerate across nerve defects.

Conduits as nerve growth structures have been developed to improve the regeneration of nerve gaps. A promising alternative seems to be the use of three-dimensional nerve conduits of different compositions for regeneration of the missing tissue [5].

Tissue engineering, combining biological knowledge, materials and engineering science, is a contemporary approach to repair and rebuild the lost tissues and organs.

In order to create a desirable environment for axonal regeneration, it is important to choose the physical, chemical, biological cues to use based on the attributes of the peripheral nerves.

An ideal nerve conduit should be, (1) thin, (2) biocompatible, (3) biodegradable, maintain its structure for at least 3 months in vivo, (4) controllable during nerve growth with regards to implantation and sterilization, (5) flexible and have the modulus of the nerve tissue to avoid compression on the regenerating nerve, (6) sufficiently strong when suturing and (7) with high porosity [6, 7].

Several methods have been used to produce porous three-dimensional scaffolds, including biopolymer replication [8–10], gas foaming [11], sintering (thermal bonding) a porous mass of particles, fibers [12], sol–gel [13], solid free form fabrication [14] and freeze-drying [15, 16]. An effective method for fabrication of porous gelatin scaffolds is freeze-drying, due to its many advantages. The main one being that it does not require high temperatures and leaching steps [17].

Gelatin, is a partial derivative of collagen, and has a wide range of uses in the pharmaceutical food and cosmetic industries [18]. The selection of gelatin as a conduit material can decrease the concerns of immunogenicity and pathogen transmission associated with collagen, since it has an almost identical composition as that of collagen [19]. For applications such as nerve tissue healing, gelatin was used as a polymer to increase the flexibility of the scaffold [20, 21]. However, it has poor mechanical properties [18, 22].

Bioceramics are often used in combination with biodegradable polymers to achieve the best possible mechanical and biological performance [20, 21]. The characteristics of nanobioglasses include excellent bioactivity, ability to deliver cells and controllable biodegradability [23]. These advantages make bioactive glasses a promising scaffold material for tissue engineering. Bioactive glasses are also being tested in applications where good interfaces are needed between soft and hard tissue. The soft tissue response may be due to their fast dissolution, which is more rapid than that for silica based glasses. It is shown that fibers of the bioglass 45S5 can form a biocompatible scaffold to guide regrowing peripheral axons in vivo [24]. In another study the magnesium in the bioglass structure is added to prevent Hydroxy-Carbonate Apatite (HCA) and is also useful for wound healing and other soft tissue applications [25].

Considering advantages of gelatin and bioglass, we have designed a novel conduit for peripheral nerve regeneration for the first time. In the present study; we investigated the suitability of a composite nerve conduit for peripheral nerve regeneration fabricated with nano bioglass and gelatin utilizing the freeze drying technique.

2 Materials and methods

2.1 Materials

0.1 M nitric acid (HNO_3), calcium nitrate ($Ca(NO_3)_2{\cdot}4H_2O$), triethyl phosphate (TEP: $C_6H_{15}O_4P$), magnesium nitrate ($Mg(NO_3)_2{\cdot}6H_2O$) and tetraethylorthosilicate (TEOS: $C_8H_{20}O_4Si$) were purchased from Merck Inc. The gelatin used in this research was purchased from Merck (microbiology grade, No. 107040) at 10 % (w/v) concentration. Also, Glutaraldehyde ($C_5H_8O_2$) solution of 25 % (w/v) was purchased from Merck Inc.

2.2 Synthesis of bioglass nanopowder

The sol–gel method was used to prepare 20–50 nm bioactive glass powder. First 13.31 ml tetraethoxysilane (TEOS) was added into 30 ml of 0.1 M nitric acid, a catalyst for hydrolysis, the mixture was allowed to react for 30 min so that the acidic hydrolysis of TEOS proceeded to near completion. The following components were added in sequence, allowing 45 min for each component to react completely: 0.91 ml triethylphosphate (TEP), 6.14 g calcium nitrate ($Ca(NO_3)_2{\cdot}4H_2O$) and 1.28 g magnesium nitrate ($Mg(NO_3)_2{\cdot}6H_2O$). After the final addition, mixing was continued for 1 h to allow the hydrolysis reaction to complete. When the gel had formed, it was dried in an oven and heated at 120 °C to remove all the water. Subsequently, the powder was milled for 10 h in a planetary mill (SVD15IG5-1, LG Company). The dry powder was heated at 700 °C for nitrate elimination. Finally, the BG nanopowder was prepared by ball milling (SVD15IG5-1, LG Company, Germany) for 30 min (Table 1).

2.3 Conduits fabrication

To engineer the nanocomposite conduits, a homogeneous aqueous solution of microbiology-grade Gelatin (GEL) (10 % weight per volume, w/v) was prepared. The

Table 1 Compositional range of the experimental glasses (wt%)

Chemical compound	TEOS (SiO_2)	TEP(P_2O_5)	$CaO(Ca(NO_3)_2{\cdot}4H_2O)$	$Mg(NO_3)_2{\cdot}6H_2O$
Mol percent (%)	64	5	26	5

synthesized BG nanopowder was added to obtain a GEL (70)/BG (30) weight percent composition. After homogenization through stirring, special mandrels were dipped in the solution several times which were subsequently frozen to solidify at −20 °C, for 3 h. To produce porous structures, the mandrels were transferred to a freeze-dryer (Christ Beta 2-8 LD plus) at −57 °C and 0.05 mbar for 24 h in order to produce a 3D porous structure through sublimation to form a gelatin network matrix on the pore walls and surface of the conduits. The emerging conduits had an internal diameter of 1.6 mm. The external diameter was found to range between 1.8–2 mm and 12 mm length. Next, the nanocomposite was soaked in a cross-linking bath of glutaraldehyde (GA) solution of 0.5 % (w/v) for 24 h to reduce biodegradation and enhance the biomechanical properties.

2.4 Characterization

2.4.1 X-ray diffraction (XRD)

Crystal structure of the nanopowder was assayed by XRD technique with CuKa = 1.54 Å wavelength (Philips, Germany). The diffractometer was operated at 40 kV and 40 mA at a 2θ range of 10–50° using a step size of 0.02° and a step time of 1 s. The BG nanopowder was analyzed by X-ray fluorescence.

2.4.2 Fourier transforms infrared spectroscopy (FTIR)

The FTIR was operated in the mid-infrared range from 400 to 4,000 cm^{-1} in reflection mode. The FTIR spectrometer was used to characterize the presence of specific chemical groups in the BG nanoparticles and the functional groups of the nanocomposite conduits. For IR analysis, 1 mg of the powder samples was carefully mixed with 300 mg of KBr (infrared grade) and palletized under vacuum. Then the pellets were analyzed at the scan speed of 120 scan min^{-1} with 4 cm^{-1} resolution.

2.4.3 Transmission electron microscopy (TEM) and scanning electron microscopy (SEM)

The particle sizes of the bioglass nanopowder were characterized using TEM (Philips, CM120, operated at 100 kV).

The scanning electron microscope photomicrographs (SEM-Philips XL30) were used to measure the average pore size of the modeled conduits. The nanocomposite samples were coated with gold using a (EMITECH K450X, England) Sputter before examination under the SEM that operated at the acceleration voltage of 15 kV. By using SEM, the cross-sectional pore size of the samples was observed.

2.4.4 Porosity measurement

Conduits porosity was calculated by the following formula [23]:

$$\%\ \text{porosity} = \frac{V_{\text{porosity}}}{V_{\text{conduit}}} \tag{1}$$

V_{Conduit} and V_{Porosity} are the conduit volume and pore volume respectively, which were calculated according to the following equation:

$$\rho = \frac{M}{V}\left(\text{g}/\text{cm}^3\right) \tag{2}$$

$$V_{\text{Prosity}} = V_{\text{conduit}} - \frac{M_{\text{gelatin}}}{\rho_{\text{gelatin}}} - \frac{M_{\text{BGpowder}}}{\rho_{\text{BGpowder}}} \tag{3}$$

V_{Conduit} is the conduit volume (cm^3), V_{BG} the actual volume of BG (cm^3), V_{Gel} the actual volume of gelatin (cm^3), V_{BG} and V_{Gel} were measured with the mass and density of BG ($\rho = 2.7$) and gelatin ($\rho = 1.35$) which were used in each sample. V_{Conduit} was determined according to the diameter and height. The total volume of each sample was 0.048 cm^3.

2.5 In vitro study

2.5.1 Cytotoxicity evaluation

Nano Bioglass/Gelatin conduits were sterilized by ethylene oxide at 38 °C and 65 % relative humidity for 8 h. After 24 h aeration in order to remove the residual ethylene oxide, the conduits were placed inside a standard 24-well-plate with culture medium being added. For cytotoxicity evaluation, culture in Dulbecco's Modified Eagle Medium (DMEM) supplemented with 10 % fetal bovine serum (FBS) and streptomycin/penicillin 100 U/ml (1 %) were added to the culture medium. Chinese hamster ovary cells with a density of 4×10^5 cell/ml were added to the samples in PS plates and maintained in an incubator (37 °C, CO_2 5 %) for 48 h [26]. The nanocomposite conduits crosslinked with GA 0.5 % (w/v) were studied for this reason. The samples were kept in 100 % ethanol for

15 min, and then visualized by light microscopy (Nikon Eclipse 50i) [27].

2.5.2 MTT detection of viable cells

The viability of the layered BG conduits in 72 h were determined by 3-(4,5-dimethylthiazol-2-yl)-2,5-diphenyl-tetrazolium bromide (MTT) assay [28]. Cytotoxicity effects of the conduits were investigated on Miapaca-2 cell lines (purchased from the Pasteur Institute, Iran). The cells were plated in 96-well culture plates at 1.7×10^4 cell/well. They were cultured in RPMI-1640 supplemented with 10 % FBS and 1 % PS in 5 % CO_2 at 37 °C. After 72 h, mediums were removed and 100 µl of fresh medium and 13 µl of MTT solutions (5 µg/ml, diluted with RPMI 1640 without phenol red) were added to each well. Incubation was allowed for another 4 h in the dark at 37 °C. Mediums were removed and 100 µl/well DMSO (dimethyl sulfoxide, Sigma, Aldrich, Germany) was added to dissolve the formazan crystals. Wells were finally read at 540 nm on an ELISA plate reader (Tecan Sunrise TM) and the percentage of viability was calculated.

The well without conduit was used as a negative control and cell viability for the MTT assay control was defined as 100 %. Each test was repeated three times.

2.6 In vivo implant preparation

All animal experiments were performed in accordance with the Ethics committee at Baqiyatallah University of medical sciences on the protection of animals used for experimental and other scientific purposes.

Adult male Wistar rats (200–250 g) were randomly divided into two groups: the normal nerve group ($n = 5$), and the BGGC group ($n = 15$).

The rats were anesthetized with a mixture of ketamine (60 mg/kg) and xylazine (10 mg/kg) given by intraperitoneal injection, and repeated as needed. The right sciatic nerve was exposed after skin incision, and the muscles around the nerve tissues were separated using blunt dissection. Subsequently, under a surgical microscope the right sciatic nerve was severed into proximal and distal segments at the center of the right thigh. Both proximal and distal stumps were secured with 8-0 nylon to a depth of 1 mm into the conduits, leaving a 10 mm gap between the stumps and the skin which was closed with 5-0 silk.

2.7 Electrophysiological assessment

To evaluate nerve regeneration, electromyographical measurements were performed 1, 2 and 3 months after surgery in both groups. The motor distal latency (DL) and the evoked muscle action potential (EMAP) of the gastrocnemius muscle were measured using an electromyographic recorder (Biomed 3250). The sciatic nerve proximal to the site of the cut was stimulated with an electric monophasic stimulus using needle electrodes. To reduce any possible interference, a ground electrode was placed inside the muscle adjacent to the nerve. The gastrocnemius response was recorded by cap electrodes placed on the gastrocnemius muscle. The distance between the site of stimulation and the muscle was 2 cm which was kept constant in the repeated studies.

2.8 Histological assessment

One, two and three months postoperatively and after the electromyography assessment, the animals were killed with an overdose of ketamine (200 mg/kg). Immediately after operation, the distal segment of the sciatic nerve was harvested and fixed in a 2 % glutaraldehyde solution at 4 °C for 12 h. Then, the nerve was dehydrated in increased concentrations of ethanol, passed through propylene oxide and embedded in Epon 812 epoxy resin. The tissue was then cut to 0.5-µm thickness by using a microtome (Leica, Germany) with a dry glass knife, stained with 0.1 % (w/v) toluidine blue. Morphometry was performed with an image analysis program Image J (http://imagej.nih.gov/ij/). Video images were obtained with a digital camera (Nikon, Ds-Fil-L2, Japan) attached to a light microscope (Nikon, 50i, Japan). By using a modified version of the Etho method, a manual count of the myelinated fibers (MFs) was performed for five randomly selected square areas (total = 0.02 mm^2) [29]. These counts were then averaged to produce a mean estimate of myelinated fibers per 1 mm^2 field.

3 Results

3.1 In vitro experiment

3.1.1 XRD analysis

Figure 1a illustrates a graph obtained from XRD analysis of bioactive glass nanopowders. The XRD pattern emphasizes the predominant amorphous state of the internal disorder and the glassy nature of the samples. It is worth mentioning that the BG does not show any crystalline state.

3.1.2 FTIR analysis

The FTIR spectrum reveals the functional groups in the conduit structure in the spectral range of 400–4,000 cm^{-1} recorded after synthesis of the nanocomposite conduits.

The FTIR spectra of BG showed vibration bands at 797 cm^{-1} and a shoulder at 1,070 cm^{-1}, which are related to the symmetric and asymmetric stretching Si–O–Si

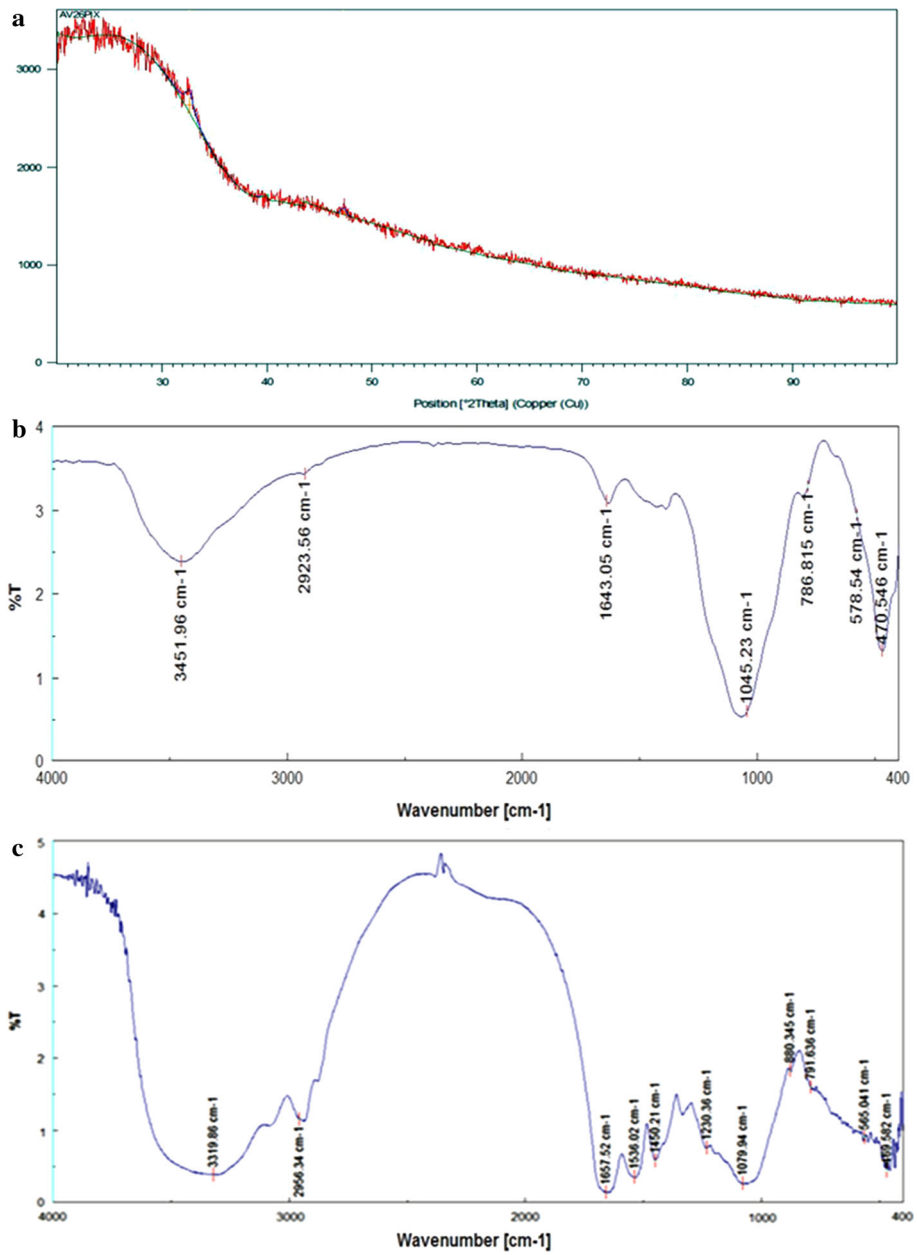

Fig. 1 The XRD pattern of the BG nanoparticles after stabilization at 700 °C (**a**), the FTIR spectra of the synthesized BG nanoparticles (**b**) and the prepared nanocomposite conduit crosslinked by GA (**c**)

bending modes. Those positioned at 1212, 930 cm^{-1} are related to the silicate network and ascribed to the LO mode of Si–O–Si and Si–O stretching of non-bridging oxygen atoms respectively (Fig. 1b).

The BG conduits also represent the FTIR spectrum of the nanocomposite that exhibited a number of new characteristic spectral bands, the most characteristics of which were protein spectrums such as: N–H bending vibration at 1,260 cm^{-1} for the amide III, N–H bending vibration at 1,560 cm^{-1} for the amide II, C=O stretching vibration at 1,670 cm^{-1} for the amide I, C–H bending vibration at 2,952 cm^{-1} for the amide B and band at 3,570 cm^{-1} indicating the presence of O–H groups, while the characteristic spectral bands for the BG nanocomposite well was present in the spectrum (Fig. 1c).

Moreover, Fig. 1c demonstrates two peaks which are related to chemical bonds that have been formed due to the appearing of new bonds after mixing of BG and gelatin and then crosslinking with GA.

$$\begin{aligned} &\mathrm{Gel{-}NH_2} + \mathrm{C_5H_8O_2} + \mathrm{NH_2{-}Gel} \\ &\longrightarrow \mathrm{Gel{-}N{=}CH - C_3H_6 - CH{=}N{-}Gel} \end{aligned} \quad (4)$$

3.1.3 Chemical bonding reaction mechanism

The first step, was an essential complex reaction between gelatin molecules and Ca^{2+} ions of the BG nanoparticles [30, 31]. In the second step, the Ca^{2+} ions of complex with gelatin molecules were assembled with PO_4^{-3} ions. The last step attached layers of gelatin molecule to the surface BG

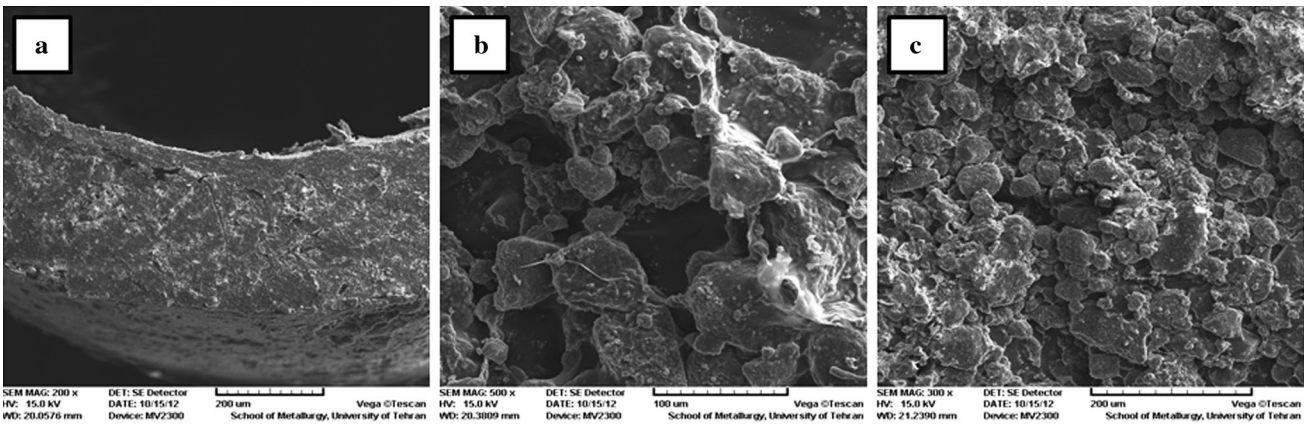

Fig. 2 SEM image of the porous nanocomposite conduit. Cross-section view of conduit (200×) (**a**), outer layer of conduit wall (500×) (**b**) and inner layer of conduit wall (300×) (**c**)

nanoparticles as the result of chemical bonding between the P–O and O–H groups of BG nanoparticles with –COOH and $–NH_2$ groups in the gelatin molecule. There are three main steps for chemical bonding between the gelatin molecule and the BG nanoparticles in the nanocomposites.

Furthermore, there are two main sources of stabilization; one is spatial stabilization and the other electrostatic stabilization which avoids nanoparticle agglomeration in these system types [32].

The spatial stabilization in this reaction system forms a thick layer on the surface of the BG nanoparticles, mainly due to the chemical absorption of gelatin molecules on the BG nanoparticles.

Electrostatic stabilization is mainly due to adsorption of Ca^{2+} ions to the surface of the BG nanoparticles in the reactions. In other words, the ionization of carboxyl is enforced while that of amino is restrained, and the carboxyl ions of gelatin are consequently against the ions in the electrical double layer.

3.1.4 TEM and SEM observations

The BG powder particle size showed particles of less than 100 nm (data not shown). These tests confirm the Nanoscale size of the synthesized BG nanoparticles.

SEM was used to observe the morphology of the nanocomposite sample. The SEM micrograph images show the porous structure of the conduit (Fig. 2).

The dense outer layer of the conduits could act as an obstacle preventing inner growth of the fibrous tissues and could also provide mechanical support and resistance to the nano-bioglass/gelatin nerve conduits. The sponge-like inner layer of the conduits could make possible the exchange of nutrition and fluids, and supply a great space for storage of the released nerve growth.

The SEM images show that the diameter of these pores vary between 10 and 40 μm which is desirable for nerve cell

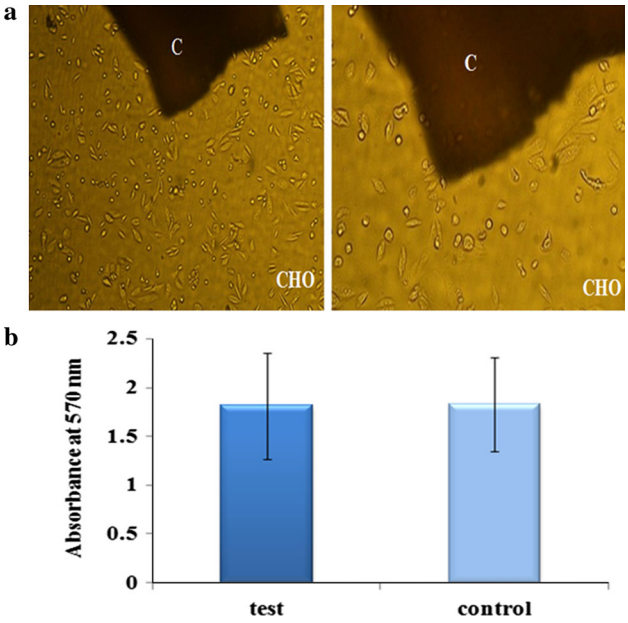

Fig. 3 Chinese hamster ovary cells cultured on the produced conduits crosslinked with 0.5 % GA (**a**) and MTT analysis results after 72 h. Groups test and control indicate disc and negative control samples, respectively. No significant differences were observed between the two test and control groups (**b**)

growth as shown in previous researches [33]. According to formula (1), the porosity was determined between 68.31 and 73.89 % with the BG nanoparticles being dispersed evenly among the cross-linked gelatin matrices.

3.2 Sample characterization after in vitro assays

3.2.1 Cytotoxicity evaluation

Figure 3a shows the pictures taken from the seeded cells on the conduit specimens. The biocompatibility of the conduits, which were cross linked with 0.5 % GA, was assessed for

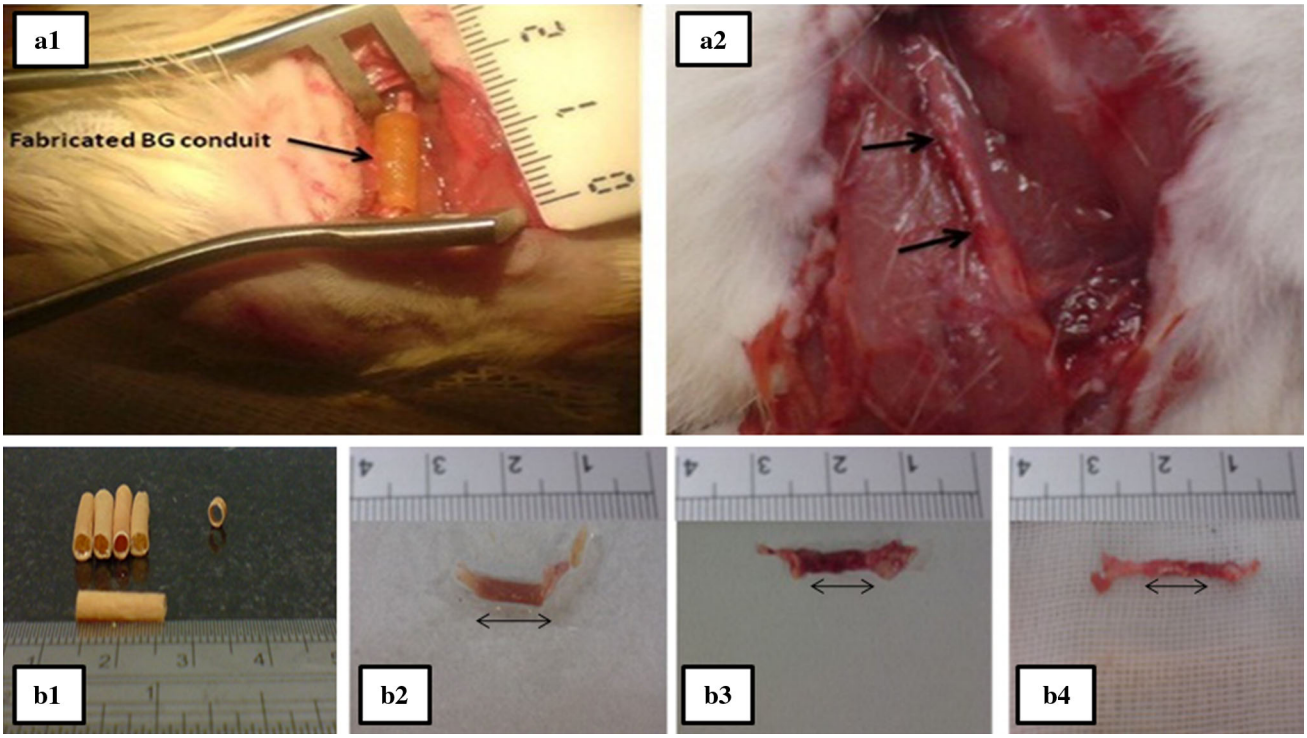

Fig. 4 Surgical implantation of a bioglass/gelatin nerve conduit bridging an 10 mm sciatic nerve defect in rats (**a**) and the view of the regenerated nerve 3 months post-surgery (**b**). Bioglass/gelatin nerve conduits prior to and after the implantation. Nano Bioglass/gelatin conduit (**b1**), 1 (**b2**), 2 (**b3**) and 3 months (**b4**) after implantation

cellular attachment, spreading and finally developing filopodias.

After 3 days of culture, the CHO cells had attached and proliferated in the surroundings of the conduit.

3.2.2 MTT detection of viable cells

MTT tests showed that cell viability of Miapaca-2 cultured in the conduit extract was not significantly different from that in the plain medium of cells during 72 h. This result clearly suggests that the fabricated conduits were nontoxic and posed as good candidates to be used as nerve conduits. The results obtained from the test and control after 72 h showed no significant cytotoxicity effects ($p > 0.05$) (Fig. 3b).

3.3 In vivo experiment

Each rat received one implant (Fig. 4 (a1)), which was removed at various time intervals: 1, 2 and 3 months, respectively. At each time interval, electrophysiological and histomorphometric evaluations were performed to evaluate the efficiency of the nano bioglass/gelatin conduits for nerve regeneration.

The animals of the BGGC groups were found to have recovered from foot ulcers on the right side with minor visible gastrocnemius muscle degeneration ($n = 15$). In the BGGC groups, the conduits were not surrounded by apparent neuroma formation or serious chronic inflammatory reaction and a thin layer of fibrous tissue abundant in capillaries. After 3 months, the bioglass/gelatin nerve conduit implanted in rats was surrounded by a thin layer of fibrous connective tissue with abundant capillaries. The original boundary areas between the conduit and nerve (black arrows) became blurry and the conduit degraded gradually as the regenerated nerve passed through (Fig. 4 (a2)).

At 1 month during the experimental period, no degradation of the BGGC was seen, for all rats. After 3 months the original boundary areas between the conduit and nerve became blurry as the regenerated nerve grew into the conduit and the conduit nearly degraded, losing its original guidance structure at the observation endpoint (Fig. 4 (a2), (b1–3)).

3.4 Electrophysiological assessment

Data comparison electrophysiology of EMAP amplitude and latency was shown in Fig. 5.

Although there was a considerable difference between the normal nerve group and the BGGC group in the first month post-surgery ($^*p < 0.05$), at three months there were

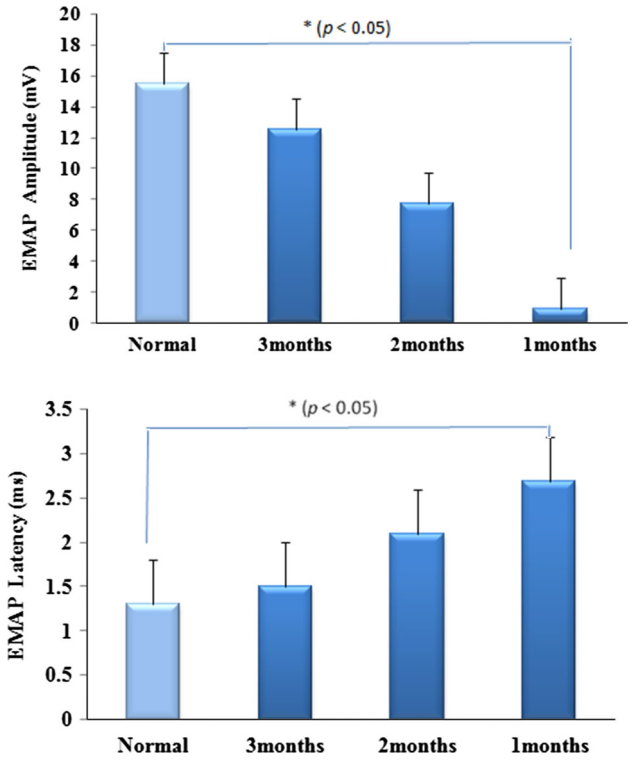

Fig. 5 Evoked muscle action potential (EMAP) detection of gastronomyus muscle 1, 2, 3 months post-surgery. Representative data of the normal nerve group and the BGGC group

statistically no significant differences between the two groups ($p > 0.05$).

3.5 Histological assessment

Figure 6 shows the regeneration process and nerve growth at 1, 2 and 3 months post-surgery, histopathology tests of the bioglass/gelatin nerve conduits indicated degradation being near completion with only a few of the residual materials being found inside the wall area 3 months postoperatively.

At first month after implantation, deformation of the BGGC was not seen. The regenerated nerves were still immature and composed of fibrin matrices, which were populated by mast cells and blood vessels (Figs. 6a, 7a (1M)). Two months after implantation, fragmentation of the BGGC continued. Regenerated units containing unmyelinated axons and Schwann cells were abundant. At 2 months, the degradation process of the tube's wall became obvious. The BGGC featured a partially fenestrated outer layer; albeit it remaining circular. Up to this time, the regenerated nerves became more mature, Schwann cells, organized in clusters, surrounding groups of unmyelinated axons were also present (Figs. 6b, 7a (2M)). After 3 months of implantation, fragmentation of the BGGC continued. Regenerated units containing axons and

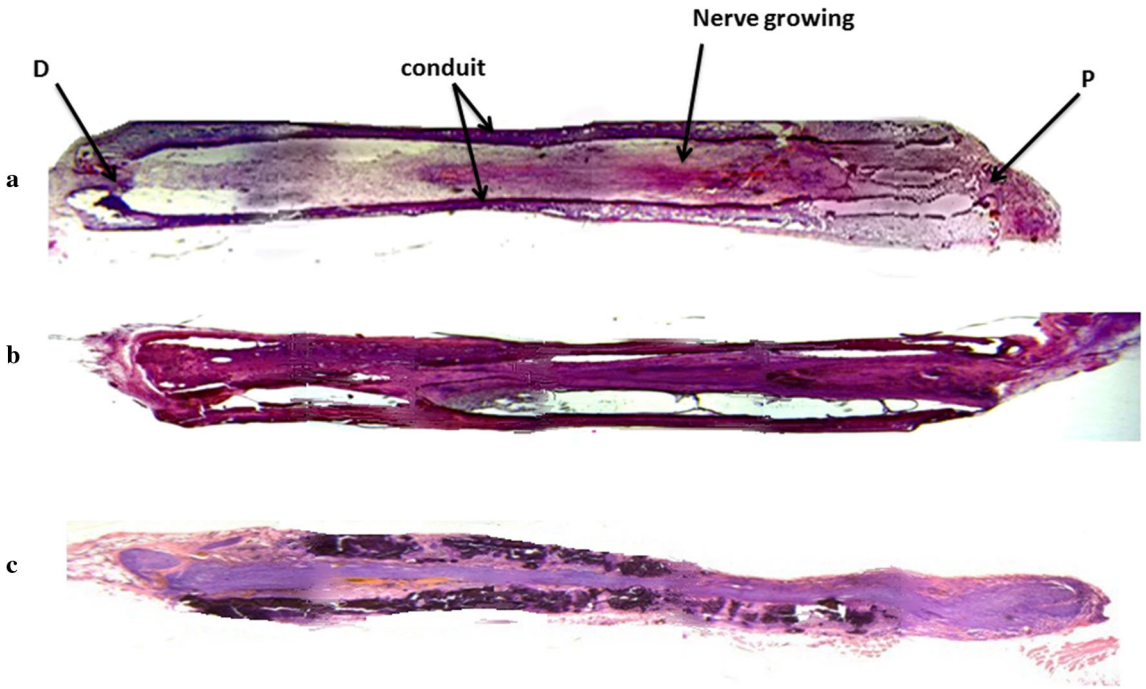

Fig. 6 Histological longitudinal section conduit after 1 (**a**), 2 (**b**) and 3 (**c**) months of surgery which represent nerve growth from proximal (P, *right*) to distal (D, *left*) and regeneration of it after 3 months (×10)

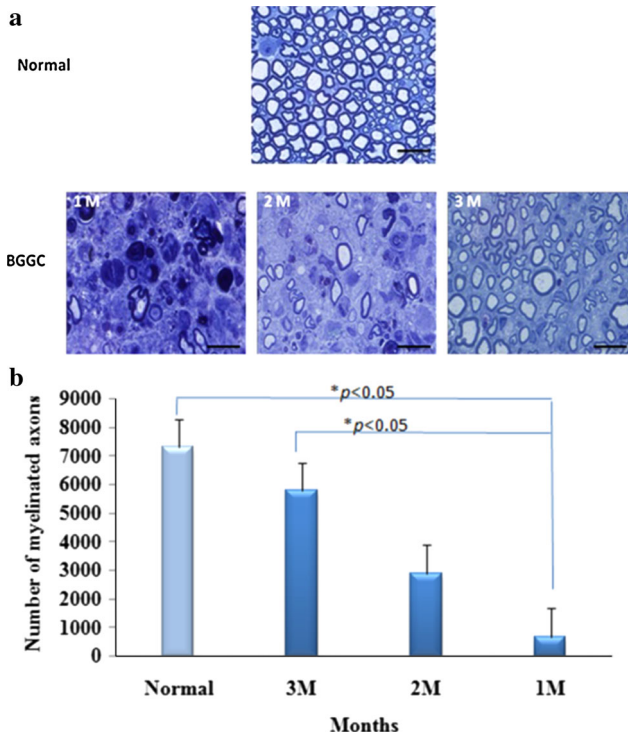

Fig. 7 Photomicrographs of semithin sections at 1 month (1M), 2 months (2M) and 3 months (3M) post-surgery in the normal and BGGC groups. Scale (*bottom right*) indicates of 20 μm (Toluidine blue staining ×100) (**a**) and number of the myelinated axons at 1 month (1M), 2 months (2M) and 3 months (3M) post-surgery (**b**)

Schwann cells were abundant (Figs. 6c, 7a (3M)). Certain small myelinated axons were interposed in the endoneurium with rich neovascularization. At 3 months, there was no difference between the data of the normal group and the conduit (BGGC) group ($p > 0.05$). At 1 and 3 months post repair of the BGGC groups, histomorphometric analysis demonstrated a statistically significant difference ($^*p < 0.05$). The average number of the myelinated fibers in different treatment groups is shown in (Fig. 7b).

4 Discussion

With peripheral nerve injuries being prevalent after traumas, autografts have been used frequently in the bridging of peripheral nerve defects. However, the limited availability and donor-site morbidity of autografts remain as inevitable drawbacks [34]. In recent times, enormous effort have been developed the synthetic nerve conduits with the different kinds of biomaterials, such as poly(L-lactide-co-glycolide) (PLGA) [35], collagen [36, 37], gelatin [38], PLGA/collagen [39], poly(L-lactic acid) (PLLA) [40]. An advantage of gelatin over collagen is its lower risk of pathogen transmittance in the nerve conduits [19]. In addition, compared to other Synthetic polymers such PLGA, PLLA it is more affordable. However gelatin has poor mechanical properties [18, 22]. Adding bioceramics such as bioglass is able to improve the mechanical features [20, 21]. The added Bioglass has a profound effect on the growth of the peripheral axons [24].

The nano bioglass/gelatin nanocomposites were prepared from a mixture of aqueous gelatin solution, with the bioactive glass being synthesized through the Sol/Gel method by freeze-drying techniques. As a bioactive nanocomposite conduit, regeneration effectiveness was investigated in a 10 mm gap in the sciatic nerve.

The XRD pattern emphasized the amorphous state and glossy nature of this material feature of the sample that the BG does not show any crystalline states. Recently reported theories by Fathi et al. [41] the amorphous structure of their nanopowder by XRD, and their results confirmed our findings.

FTIR microscopy has proven to be a powerful tool to characterize the presence of various chemical groups. Our diagram shows the FTIR spectra for the BG nanoparticles and scraped material surfaces of the nanocomposite conduit in the 400–4,000 cm^{-1} spectral range. The band located at 609 cm^{-1} is attributed to the asymmetric vibration of PO_4^{3-} [42].

In previous studies for gelatin and hydroxyapatite that the first one at about 1,359 cm^{-1} indicates the formation of the chemical bond between carboxyl groups from gelatin and Ca^{2+} ions from the BG [8, 43]. The second band at 2,349 cm^{-1} appeared after crosslinking of gelatin with GA as mentioned former by Azami et al. (Fig. 6) [8].

TEM micrograph of the synthesized BG particles showed certain agglomeration of the nanopowders due to their high surface area. The results also confirmed that the particles clearly had sizes less than 100 nm. Mortazavi et al. [43] and Mozafari and associates [44] reported the sizes of their synthetic BG particles to be in the range of nano.

The SEM micrograph images showed a porous structure in the dense outer layer and the inner layer of the conduit, conforming with the SEM results of Yumin Yang et al. [45].The SEM images indicate a well-distributed porous structure in the conduits with pore sizes around 10–40 μm with the conduits porosity being between 68.31 and 73.89 % according to the mentioned formula (1) Our result is conforming with Nojehdehian et al. [33] and Chang et al. [35] who synthesized their conduits utilizing poly-L-lysine coated with PLGA and poly(DL-lactic acid-co-glycolic acid).

To investigate the biocompatibility of the produced conduits, Chinese hamsters cells cultivated under DMEM environment were used. After 72 h of culture, the CHO cells had attached and proliferated around the conduit, confirming with the illustration by Lu et al. [46] that the bioglass composite had no cytotoxicity. The data obtained from MTT analysis showed no cytotoxic effects on the viability

and proliferation properties of the cells during 72 h. Soňa Jantová and colleagues reported that the bioglass scaffold had a slight cytotoxicity and was biocompatible [47]. Therefore their data confirmed our data in this regards.

As a result, we found that successful regeneration of the nerves across the gap occurred in all of the nano bioglass/gelatin conduits even at the shortest experimental time point of 1 month. The thin layer of the surrounding fibrous tissue and the minimal inflammation also indicated that the nano bioglass/gelatin conduit were biocompatible. These results are not surprising since gelatin and bioglass have both been shown to be biocompatible materials [24, 48].

Regeneration of the myelinated axons was observed in the distal segment of all groups. The mean number of the myelinated fibers was used as a parameter for morphometry. In the BGGC group, rats presented a greater mean number at 3 months compared to those from 1 and 2 months. At 3 months, no significant difference was observed between the BGGC and normal group. Our result is conforming with Yueh-Sheng Chen et al. [38].

Measurements of peak amplitude and latency both showed an increase as a function of the experimental period, which suggested that the transected nerve had undergone adequate regeneration and was approximately near to the normal group. Our result is conforming with Wenwen associates [49].

On the other hand, since rats display regeneration in the peripheral nervous system superior to that in humans, the results of this study can be used as a starting point for further investigations in higher species, for example, in dogs or cats [50, 51].

5 Conclusion

According to our study, the nano-bioglass/gelatin conduit could be a suitable candidate for peripheral nerve regeneration as a biocompatible, biodegradable and novel biomaterial.

Acknowledgments This work was supported by the grant from the Nano biotechnology research center of Baqiyatallah University of Medical Sciences and Iranian National Sciences foundation (INSF).

References

1. Moore MJ, Friedman JA, Lewellyn EB, Mantila SM, Krych AJ, Ameenuddin S, et al. Multiple-channel scaffolds to promote spinal cord axon regeneration. Biomaterials. 2006;27:419–29.
2. Prang P, Muller R, Eljaouhari A, Heckmann K, Kunz W, Weber T, et al. The promotion of oriented axonal regrowth in the injured spinal cord by alginate-based anisotropic capillary hydrogels. Biomaterials. 2006;27:3560–9.
3. Amillo S, Yáñez R, Barrios RH. Nerve regeneration in different types of grafts: experimental study in rabbits. Microsurgery. 1995;16:621–30.
4. Balgude AP, Yu X, Szymanski A, Bellamkonda RV. Agarose gel stiffness determines rate of DRG neurite extension in 3D cultures. Biomaterials. 2001;22:1077–84.
5. Chang JY, Lin JH, Yao CH, Chen JH, Lai TY, Chen YS. In vivo evaluation of a biodegradable EDC/NHS-cross-linked gelatin peripheral nerve guide conduit material. Macromol Biosci. 2007;7:500–7.
6. Pfister LA, Christen T, Merkle HP, Papaloïzos M, V B. Novel biodegradable. Novel biodegradable nerve conduits for peripheral nerve regeneration. Eur Cells and Mater. 2004;7:16–7.
7. Verreck G, Chun I, Li Y, Kataria R, Zhang Q, Rosenblatt J, et al. Preparation and physicochemical characterization of biodegradable nerve guides containing the nerve growth agent sabeluzole. Biomaterials. 2005;26:1307–15.
8. Azami M, Moztarzadeh F, Tahriri M. Preparation characterization and mechanical properties of controlled porous gelatin/hydroxyapatite nanocomposite through layer solvent casting combined with freeze-drying and lamination techniques. Porous Mater. 2009;17:313–20.
9. Lutolf MP, Hubbell JA. Synthetic biomaterials as instructive extracellular microenvironments for morphogenesis in tissue engineering. Biotechnology. 2005;23:74–5.
10. Lawrencin CT, Amin SFE, Ibim SE, Willoughby DA, Attavia M, Allcock HR, et al. A highly porous 3-dimensional polyphosphazene polymer matrix for skeletal tissue regeneration. J Biomed Mater Res. 1996;30:133–8.
11. Yuan H, De Bruijn JD, Zhang X, Bitterswijk CAV, De Groot K. Factors affecting the structure and properties of bioactive foam scaffolds for tissue engineering. J Biomed Mater Res. 2008;68:270–6.
12. Huang ZM, Zhang YZ, Ramakrishna S, Lim CT. Electrospinning and mechanical characterization of gelatin nanofibers. Polymer. 2004;45:5361–8.
13. Jones JR, Ahir S, Hench LL. Large-scale production of 3D bioactive glass macroporous. Sol-Gel Sci Technol. 2004;29:179–88.
14. Taboas JM, Maddox RD, Krebsbach PH, Hollister SJ. Indirect solid free form fabrication of local and global porous, biomimetic and composite 3D polymer-ceramic scaffolds. Biomaterials. 2003;24:181–94.
15. Carrasquillo KG, Stanley AM, Aponte-Carro JC, De Jesus PDJ, Costantino HR, Bosques CJ. Non-aqueous encapsulation of excipient-stabilized spray freeze dried BSA into poly(lactide-co-glycolide) microspheres results in release of native protein. Control Release. 2001;76:199–208.
16. Fu H, Fu Q, Zhou N, Huang W, Rahaman MN, Wang D, et al. In vitro evaluation of borate-based bioactive glass scaffolds prepared by a polymer foam replication method. Eng Mater Sci Lett. 2009;29:2079–312.
17. Boland ED, Espy P, Bowlin GL. Tissue engineering scaffolds. In: Encyclopaedia of Biomaterials and biomedical engineering. 2004. p. 1633–5.
18. Boedtker H, Doty PA. A study of gelatin molecules aggregates and gels. J Phys Chem. 1954;58:968–83.
19. Gardin C, Ferroni L, Favero L, Stellini E, Stomaci D, Sivolella S, et al. Nanostructured biomaterials for tissue engineered bone tissue reconstruction. Int J Mol Sci. 2012;13:737–57.
20. Rezwan K, Chen QZ, Blaker JJ, Boccaccini AR. Biodegradable and bioactive porous polymer/inorganic composite scaffolds for bone tissue engineering. Biomaterials. 2006;27:3413–31.
21. Guarino V, Causa F, Ambrosio L. Bioactive scaffolds for bone and ligament tissue. Expert Rev Med Devices. 2007;4:405–18.
22. Liu X, Smith LA, Hu J, Ma PX. Biomimetic nanofibrous gelatin/apatite composite scaffolds for bone tissue engineering. Biomaterials. 2009;30:2252–8.
23. Mozafari M, Moztarzadeh F, Rabiee M, Azami M, Maleknia S, Tahriri M, et al. Development of macroporous nanocomposite

scaffolds of gelatin/bioactive glass prepared through layer solvent casting combined with lamination technique for bone tissue engineering. Ceram Int. 2010;36:2431–9.
24. Bunting S, Silvio LD, Deb S, Hall S. Bioresorbable glass fibres facilitate peripheral nerve regeneration. Hand Surgery. 2005;30: 242–7.
25. Jones JR. Review of bioactive glass: from Hench to hybrids. Acta Biomater. 2013;9:4457–86.
26. Picot J. Human cell culture protocol. CA, USA; 2004.
27. Fassina L, Saino E, Visai L, Avanzini MA, Cusella De Angelis MG, Benazzo F, Van Vlierberghe S, Dubruel P, Magenes G. Use of a gelatin cryogel as biomaterial scaffold in the differentiation process of human bone marrow stromal cells. Conf Proc IEEE Eng Med Biol Soc. 2010;247–50. doi:10.1109/IEMBS.2010.5627475.
28. Hafezi F, Hosseinnejad F, Fooladi AA, Mohit Mafi S, Amiri A, Nourani MR. Transplantation of nano-bioglass/gelatin scaffold in a non-autogenous setting for bone regeneration in a rabbit ulna. J Mater Sci Mater Med. 2012;23:2783–92.
29. Eto M, Yoshikawa H, Fujimura H, Naba I, Sumi-Akamaru H, Takayasu S, et al. The role of CD36 in peripheral nerve remyelination after crush injury. Eur J Neurosci. 2003;17:2659–66.
30. Teng S, Shi J, Peng B, Chen FL. The effect of alginate addition on the structure and morphology of hydroxyapatite/gelatin Nanocomposites. Compos Sci Technol. 2006;66:1532–8.
31. Chang MC, Ko CC, Douglas WH. Conformational change of hydroxyapatite-gelatin nanocomposite by glutaraldehyde. Biomaterials. 2003;24:3087–94.
32. Minfang C, Junjun T, Yuying L, Debao L. Preparation of gelatin coated hydroxyapatite nanorods and the stability of its aqueous colloidal. Appl Surf Sci. 2008;254:2730–5.
33. Nojehdehian H, Moztarzadeh F, Baharvand H, Nazarian H, Tahriri M. Preparation and surface characterization of poly-L-lysine-coated PLGA microsphere scaffolds containing retinoic acid for nerve tissue engineering: in vitro study. Colloids Surf B Biointerfaces. 2009;73:23–9.
34. Bian YZ, Wang Y, Aibaidoula G, Chen GQ, Wu Q. Evaluation of poly(3-hydroxybutyrate-co-3-hydroxyhexanoate) conduits for peripheral nerve regeneration. Biomaterials. 2009;30:217–25.
35. Chang C-J, Hsu S-H. The effect of high outflow permeability in asymmetric poly(DL-lactic acid-co-glycolic acid) conduits for peripheral nerve regeneration. Biomaterials. 2006;27:035–1042.
36. Ahmed MR, Vairamuthu S, Shafiuzama M, Basha SH, Jayakumar R. Microwave irradiated collagen tubes as a better matrix for peripheral nerve regeneration. Brain Res. 2005;1046:55–67.
37. Schnell E, Klinkhammer K, Balzer S, Gary B, Doris K, Paul D, et al. Guidance of glial cell migration and axonal growth on electrospun nanofibers of poly-epsilon-caprolactone and a collagen/poly-epsilon-caprolactone blend. Biomaterials. 2007;28: 3012–25.
38. Chen YS, Chang J, Cheng CY, Tsai FJ, Yao CH, Liu BS. An in vivo evaluation of a biodegradable genipin-cross-linked gelatin peripheral nerve guide conduit material. Biomaterials. 2005;26: 3911–8.
39. Liu B, Cai SX, Ma KW, Xu ZL, Dai XZ, Yang L, Lin C, Fu XB, Sung KL, Li XK. Fabrication of a PLGA-collagen peripheral nerve scaffold and investigation of its sustained release property in vitro. J Mater Sci Mater Med. 2008;19:1127–32.
40. Evans JR, Brandt K, Katz S, Chauvin P, Otto L, Bogle M. Bioactive poly(L-lactic acid) conduits seeded with Schwann cells for peripheral nerve regeneration. Biomaterials. 2002;23:841–8.
41. Fathi MH, Mortzavi VA, Doostmohammadi A. Bioactive glass nanopowder for the treatment of oral bone defects. Dentistry. 2007;4:115–22.
42. Mami M, Lucas-Girot A, Oudadesse H, Dorbez-Sridi R, Mezahi F, Dietrich E, et al. Investigation of the surface reactivity of a sol gel derived glass in the ternary system SiO_2-CaO-P_2O_5. Appl Surf Sci. 2008;254:7386–93.
43. Mortazavi V, Nahrkhalaji MM, Fathi MH, Mousavi SB, Esfahani BN. Antibacterial effects of sol-gel-derived bioactive glass nanoparticle on aerobic bacteria. Biomed Mater Res A. 2010;94: 160–8.
44. Masoud M, Rabiei M, Azami M, Maleknia S. Biomimetic formation of apatite on the surface of porous gelatin/bioactive glass nanocomposite scaffolds. Appl Surf Sci. 2010;257:1740–9.
45. Yang Y, Zhao W, He J, Zhao Y, Ding F, Gu X. Nerve conduits based on immobilization of nerve growth factor onto modified chitosan by using genipin as a crosslinking agent. Pharm Biopharmaceutics. 2011;79:519–25.
46. Lu HH, El-Amin SF, Scott KD, Laurencin CT. Three-dimensional, bioactive, biodegradable, polymer-bioactive glass composite scaffolds with improved mechanical properties support collagen synthesis and mineralization of human osteoblast-like cells in vitro. Biomed Mater Res A. 2003;64:465–74.
47. Jantová S, Theiszová M, Matejov P, Bakoš D. Biocompatibility and cytotoxicity of bioglass-ceramic composite with various P_2O_5 content in Li_2O-SiO_2-CaO-CaF_2-P_2O_5 system on fibroblast cell lines. Acta Chimica Slovaca. 2011;4:15–30.
48. Mligiliche NL, Tabata Y, Ide C. Nerve regeneration through biodegradable gelatin conduits in mice. East Afr Med J. 1999;76: 400–6.
49. Yu W, Zhau W, Zhu C, Zhang X, Ye D, Zhang W, et al. Sciatic nerve regeneration in rats by a promising electrospun collagen/poly(ε-caprolactone) nerve conduit with tailored degradation rate. Neuroscience. 2011;12:1471–2202.
50. Peker F, Solakoglu C, Yuksel F, Kutlay M. Effects of time lapse on results of partial nerve injury repair. J Reconstr Microsurg. 2005;21:145–9.
51. Sinis N, Schulte-Eversum C, Doser M, Müller HW. Nerve regeneration across a 2-cm gap in the rat median nerve using a resorbable nerve conduit filled with Schwann cells. J Neurosurg. 2005;103:1067–76.